Available online at www.sciencedirect.com
SCIENCE DIRECT
Journal of Colloid and Interface Science 299 (2006) 305–320
JOURNAL OF Colloid and Interface Science
www.elsevier.com/locate/jcis

Adsorption of reactive dyes on titania–silica mesoporous materials

Paula V. Messina *, Pablo C. Schulz

Departamento de Química, Universidad Nacional del Sur, 8000 Bahía Blanca, Argentina

Received 3 December 2005; accepted 19 January 2006
Available online 23 March 2006

Abstract

This paper presents a study on the adsorption of two basic dyes, methylene blue (MB) and rhodamine B (RhB), from aqueous solution onto mesoporous silica–titania materials. The effect of dye structure, adsorbent particle size, TiO_2 presence, and temperature on adsorption was investigated. Adsorption data obtained at different solution temperatures (25, 35, and 45 °C) revealed an irreversible adsorption that decreased with the increment of T. The presence of TiO_2 augmented the adsorption capacity (q_e). This would be due to possible degradation of the dye molecule in contact with the TiO_2 particles in the adsorbent interior. The adsorption enthalpy was relatively high, indicating that interaction between the sorbent and the adsorbate molecules was not only physical but chemical. Both Langmuir and Freundlich isotherm equations were applied to the experimental data. The obtained parameters and correlation coefficients showed that the adsorption of the two reactive dyes (MB and RhB) on the adsorbent systems at the three work temperatures was best predicted by the Langmuir isotherm, but not in all cases. The kinetic adsorption data were processed by the application of two simplified kinetic models, first and second order, to investigate the adsorption mechanism. It was found that the adsorption kinetics of methylene blue and rhodamine B onto the mesoporous silica–titania materials surface under different operating conditions was best described by the first-order model.

Keywords: Adsorption; TiO_2 nanoparticles; Silica–titania mesoporous materials; Surfactant templates; Reactive dyes; Energetic surface heterogeneity; Decontamination; Isotherms; Kinetics; Thermodynamic

1. Introduction

Colored organic effluents are produced in the textile, paper, plastic, leather, food, and mineral processing industries [1]. Wastewater containing pigments and/or dyes can cause serious water pollution problems.

Reactive dyes are the largest single group of dyes used in industry. Being highly water-soluble, it is estimated that 10–20% of reactive dye remains in wastewater during the production [2] of these dyes and nearly 50% of reactive dyes may be lost to the effluents during dyeing of cellulose fibers [3]. Such highly colored wastes not only are aesthetically displeasing but also hinder light penetration and may in consequence disturb biological processes in water bodies. In addition, dyes are toxic to some organisms and hence harmful to aquatic animals.

Furthermore, the expanded uses of dyes have shown that some of them and their reaction products, such as aromatic amines, are highly carcinogenic [4,5]. Therefore, removal of dyes before disposal of wastewater is necessary.

Reactive dye wastewater is characterized by poor biodegradability, thus conventional wastewater treatment is not suitable [6]. Other approaches, such as flocculation, chemical oxidation, membrane separation, and adsorption, have gained favor due to their efficiency and relatively simple equipment.

A wide variety of materials, such as clay minerals [7], activated carbon, bagasse pith [8], wood [9], maize cob [10], and peat [11], are being evaluated as viable adsorbents to remove dyes from colored effluents.

Semiconducting titania materials are currently attracting attention due to their marked photocatalytic effect in removing pollutants [12–14].

TiO_2 exists in three different crystalline phases: anatase, rutile and brookite [15,16]. Although both rutile and anatase have been studied for their photocatalytic activity, anatase is generally more active in photocatalysis than rutile [17].

* Corresponding author. Fax: +54 291 4551447.
E-mail address: pau423ve@yahoo.com.ar (P.V. Messina).

0021-9797/$ – see front matter
doi:10.1016/j.jcis.2006.01.039

Anatase titania nanocrystals were obtained by the cooperative self-assembly of surfactants to wrap titania particles once. The combination of anatase titania nanocrystals with mesopores leads to the construction of nanostructured titania film with mesostructure, larger surface area, and quantum size effects [17].

It is advantageous for pollutants to react on the surface of mesoporous titania films, and diffuse within the mesopores for heterogeneous photocatalytic reaction.

In this work, adsorption on titania–silica mesoporous materials from aqueous reactive dye solutions has been studied. The focus in the present research is on characterizing the sorption properties of these materials.

Titania mesosized particles were obtained by $TiCl_4$ hydrolysis in aerosol OT/water/*n*-hexane emulsion and then incorporated into surfactant templated silica mesoporous materials of MCM-41 and MCM-50 structures. Their syntheses were reported in a previous work [18].

2. Experimental

In this study three different mesoporous silica–titania materials were used: hexadecyltrimethylammonium bromide template material (HTAB + TiO_2), which retained the honeycomb structure of the MCM-41, and dodecyltrimethylammonium bromide (DTAB + TiO_2) and didodecyldimethylammonium (DTAB + TiO_2) template materials, which had a lamellar structure. Materials syntheses and surface, and porosity characterizations were described in a previous work [18].

The synthesis of TiO_2 nanoparticles was via an inverse AOT/hexane/water microemulsion. The silica: titania (4:1) materials were prepared by addition of dry AOT–TiO_2 material obtained without calcination to the surfactant solution (HTAB, DTAB, or DDAB) in water and then sonicated to complete material suspension. The resulting solution was added to a tetraethylorthosilicate (TEOS) solution. The system was treated as common MCM-41 material [19].

As adsorbates, two cationic dyes, methylene blue (MB) and rhodamine B (RhB), were chosen.

MB is a basic blue dyestuff, CI classification number 52015. The chemical formula is $C_{16}H_{18}NSCl$; molar weight 373.9 g/mol. RhB is a basic dye, $C_{28}H_{31}ClN_2O_3$, molar weight 479.02 g/mol. For reference, the dye structures are shown in Fig. 1.

All reagents were obtained from Aldrich and were of analytical grade. Both dyes were utilized without further treatment. For aqueous dye solutions only double-distilled water was used.

Adsorption experiments were carried out in 5-ml glass-stoppered round-bottom flasks immersed in a thermostatic shaker bath. For this 50 mg of adsorbent was mixed with 5 ml of aqueous dye solutions of (0.1–2.5) mmol/L concentration range. The flasks with its contents were then shaken for the different adsorption times at 25, 35, and 45 °C. In the experiments, the stirring speed was kept constant at 90 rpm. At the end of adsorption period, the supernatant was centrifuged for 1 min at a speed of 3000 min^{-1}.

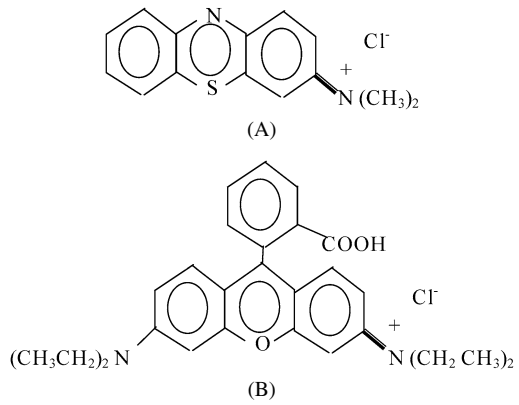

Fig. 1. Molecular structure of (A) methylene blue, (B) rhodamine B.

Table 1
Characteristics of the adsorbents are A_{BET}, BET surface area; A_{tmp}, *t*-plot micropore; A_{text}, *t*-plot external surface; D_{aap}, adsorption average pore diameter by BET

Adsorbent system	A_{BET} (m^2/g)	A_{tmp} (m^2/g)	A_{text} (m^2/g)	D_{aap} (nm)	Structure	Wall thickness (nm)
HTAB + TiO_2	272.38	7.85	264.53	6.61	Honeycomb	0.31
DTAB + TiO_2	55.95	17.29	38.65	9.54	Lamellar + granular	4.31
DDAB + TiO_2	43.35	4.07	39.27	9.67	Lamellar	4.88
HTAB	238.6			4.55	Honeycomb	0.91
DDAB	17.32	3.30	14.02	5.75	Lamellar	3.86

The concentration of MB and RhB in the supernatant before and after adsorption was determined using a Spectronic-20 UV–vis spectrophotometer at 661 and 543 nm, respectively.

3. Results and discussion

Adsorbent structure analysis, mesopore size distribution, and surface area determination were done in a previous work [18]. Several of the obtained results are shown in Table 1.

3.1. Adsorption isotherm

An adsorption isotherm describes how adsorbates interact with adsorbents. Thus, the correlation of equilibrium data by either a theoretical or an empirical equation is essential to the practical design and operation of an adsorption system.

Two isotherm equations are tested in this work. One is the Langmuir isotherm equation, which has been widely applied to describe experimental adsorption data based on the assumption that maximum adsorption corresponds to a saturated monolayer of adsorbate molecules on the adsorbent surface with constant energy and no transmigration of adsorbate in the plane of adsorbent surface. The theoretical Langmuir isotherm equation can be represented as [20]

$$q_e = \frac{q_{mon} K_L C_e}{1 + K_L C_e}, \tag{1}$$

where K_L is the Langmuir constant related to the energy of adsorption and q_{mon} is the maximum amount of adsorption

corresponding to complete monolayer coverage on the surface.

The equilibrium adsorption capacity, q_e (mg/g), was calculated with the equation [21]

$$q_e = \frac{(C_0 - C_e)V}{m}, \tag{2}$$

where C_0 is the initial concentration (mg/L), C_e the residual concentration at equilibrium (mg/L), V the solution volume (L), and m the adsorbent mass (mg).

The constants K_L and q_{mon} can be determined from the following linearized form of Eq. (1),

$$\frac{1}{q_e} = \frac{1}{q_{mon}} + \frac{1}{K_L q_{mon}} \frac{1}{C_e}. \tag{3}$$

The Freundlich isotherm [21] is the earliest known relationship describing the sorption equation. This fairly satisfactory empirical isotherm can be used for nonideal sorption that involves heterogeneous surface energy systems and is expressed by the equation

$$q_e = K_F C_e^{1/n}, \tag{4}$$

where K_F is roughly an indicator of adsorption capacity and $1/n$ is the adsorption intensity. In general, as K_F increases the adsorption capacity of an adsorbent for a given adsorbate increases. The magnitude of the exponent $1/n$ gives an indication of the favorability of adsorption. The Freundlich equation can be derived from the Langmuir one by supposing that the variation in $\theta = q_e/q_{mon}$ and K_L may be attributed entirely to variation in the heat of adsorption ΔH_{ads} because of the heterogeneity of the adsorbent surface [22].

Equation (4) may be linearized by taking logarithms:

$$\log q_e = \log K_F + \frac{1}{n} \log C_e. \tag{5}$$

In order to determine the mechanism of dye adsorption and evaluate the effect of temperature on adsorption capacity, the experimental data, Figs. 2–5, were represented following Langmuir and Freundlich isotherm equations.

The adsorption capacity variation vs concentration for the different adsorption systems is shown in Figs. 2 and 3.

The parameters and correlation coefficients calculated for the models are given in Tables 2 and 3.

From the obtained data, it was clear that dyes' adsorption mechanisms depend on the adsorbent structure, on the dyes molecular structure, and on the temperature.

To determine which of the adsorption isotherms better represents the experimental data, the difference between correlation coefficients ($\Delta r = r_{Langmuir} - r_{Freundlich}$) was fitted as a function of temperature for both dyes in Figs. 6 and 7. In general it may be seen that Δr is positive, which means that the Langmuir representation is better than the Freundlich one, but there are some exceptions, and the temperature dependence of Δr also varies with the kind of adsorbent and the dye nature.

For both MB and RhB, Δr is positive for adsorption on the material synthesized with HTAB + TiO_2 at 25 and 35 °C but negative at 45 °C. The same behavior may be seen in the adsorption on the DTAB + TiO_2 templated material.

For the DDAB + TiO_2 templated material, the behavior is different. For the adsorption of RhB, Δr is negative at 25 °C, and thus the Freundlich adsorption isotherm is favored, but becomes strongly positive at higher temperatures. For MB Δr is always positive and has a maximum at 35 °C.

For the HTAB without addition of titania-templated material, Δr is always positive and insensitive to temperature changes for RhB adsorption, while MB shows a small dependence on temperature, being positive at 25 °C and negative at higher temperatures. For the adsorbent templated with DDAB without addition of titania, Δr is always positive for both dyes and only slightly dependent on temperature.

When Δr is positive, the formation of a monolayer (but not necessarily a compact one) may be assumed and the thermodynamic data obtained from the Langmuir equation are trustworthy. When Δr is negative the Freundlich equation fits the data better. This means that the adsorbent surface is not homogeneous and that the different adsorption sites at the surface are not energetically equivalent, which is in agreement with the presence of both SiO_2 and TiO_2 groups in the adsorbent structure. It also must be taken into account that both oxides may be ionized (e.g., silica may be as siliceous acid) or not.

For the HTAB + TiO_2 and DTAB + TiO_2 templated materials the inversion in the sign of Δr may be associated with the expositing of heterogeneous surface groups to the dyes when temperature increases. This may be caused by a combination of pore diameter expansion, surface group hydrolysis, and increase of dye diffusivity and/or reactivity. The adsorption behavior of MB on the adsorbent templated with HTAB and without titania suggests that the latter factor may be the main explanation. RhB adsorption is almost insensitive and it cannot enter into the small pores of this adsorbent (see below), whereas the HTAB + TiO_2 adsorbent has larger pores and probably allows the penetration of the dye into the pores.

The behavior in the DDAB + TiO_2 templated material is rather different: Δr for RhB indicates that the Freundlich isotherm is a better fit to the data at 25 °C, but Langmuir becomes better when the temperature is increased. Because the lamellar structure makes it improbable that the surface exposed to adsorption increases with temperature, exposing new adsorption sites, a possible explanation may be that the difference in adsorption energy between the different sites is not very great and becomes negligible when the thermal energy increases. This possible interpretation is supported by the fact that Δr is almost insensitive to the temperature in the DDAB templated system without added titania.

As a consequence of this discussion, the thermodynamic data of the systems having an inversion of the Δr sign must be considered as average values.

Lamellar structure materials with and without titania presented higher adsorption with respect to the honeycomb structure adsorbents. The presence of TiO_2 particles in the honeycomb structure material increased the dye adsorption at all temperatures. Comparing the results obtained from the MB adsorption experiments on adsorbents with and without titania

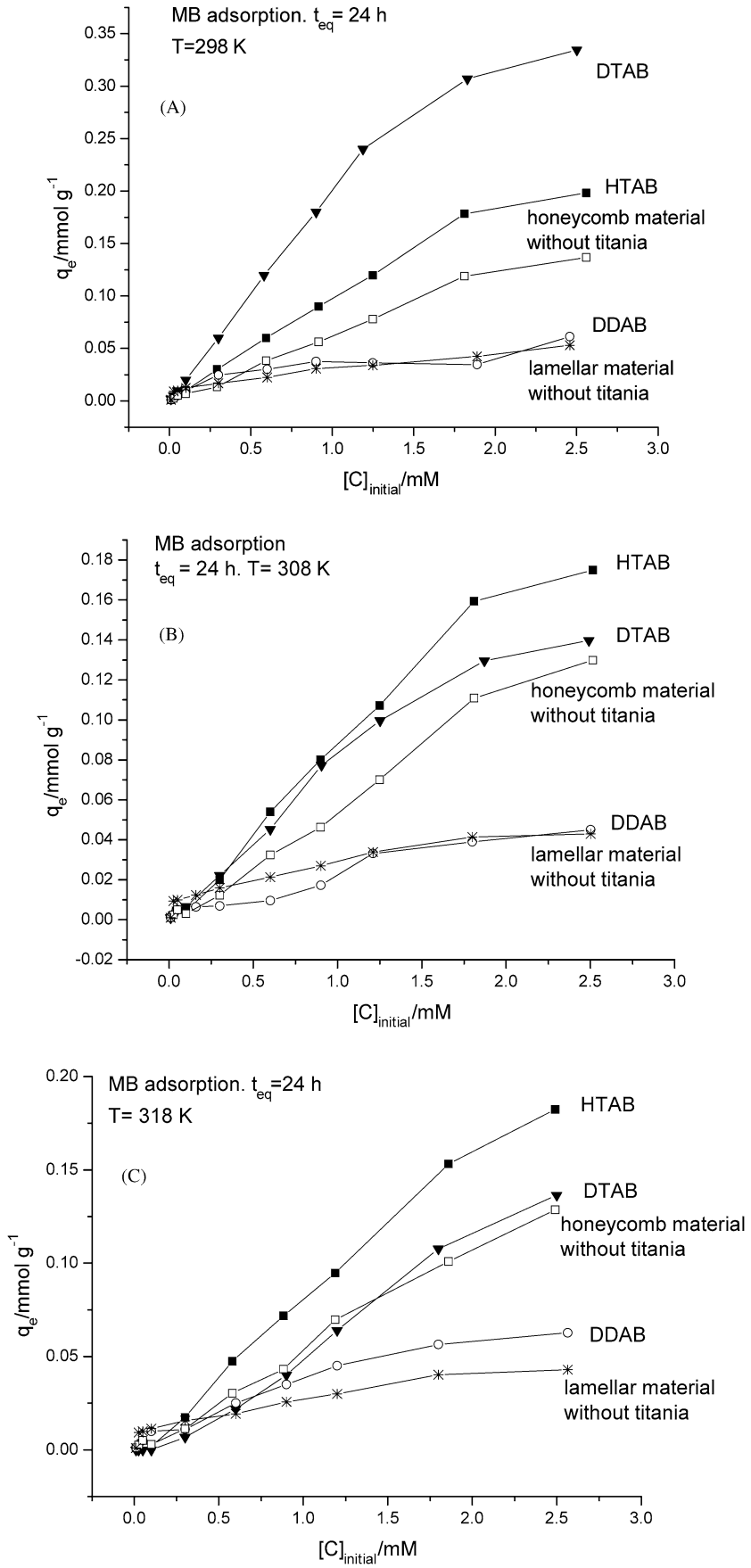

Fig. 2. Adsorption isotherms of methylene blue (MB) at (A) 25, (B) 35, and (C) 45 °C. Adsorbent materials templated with (▼) DTAB, (■) HTAB, and (○) DDAB, (∗) mesoporous DDAB-templated lamellar silica material without titania, (□) mesoporous silica honeycomb material synthesized with HTAB without titania.

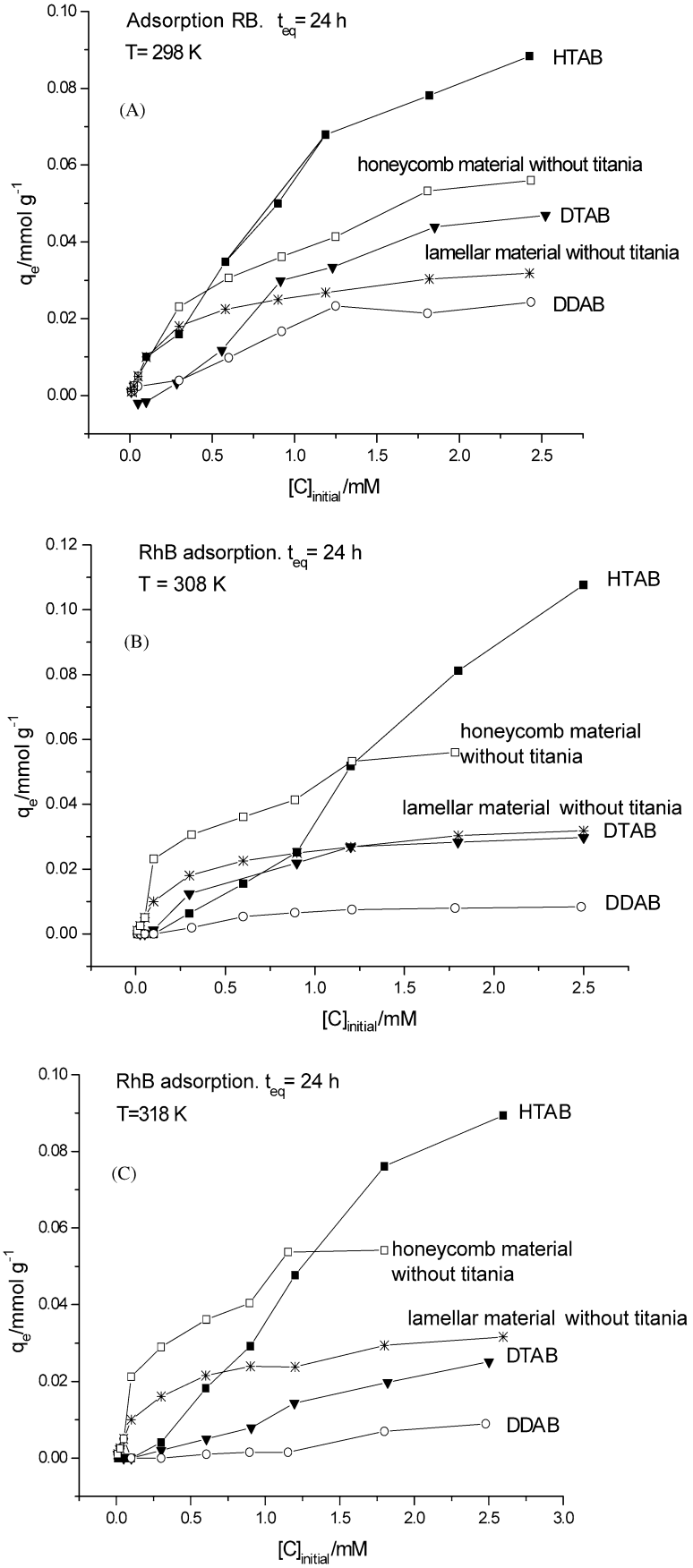

Fig. 3. Adsorption isotherms of rhodamine B (RhB) at (A) 25, (B) 35, and (C) 45 °C. Adsorbent materials templated with (▼) DTAB, (■) HTAB, and (○) DDAB, (∗) mesoporous DDAB-templated lamellar silica material without titania, (□) mesoporous silica honeycomb material synthesized with HTAB without titania.

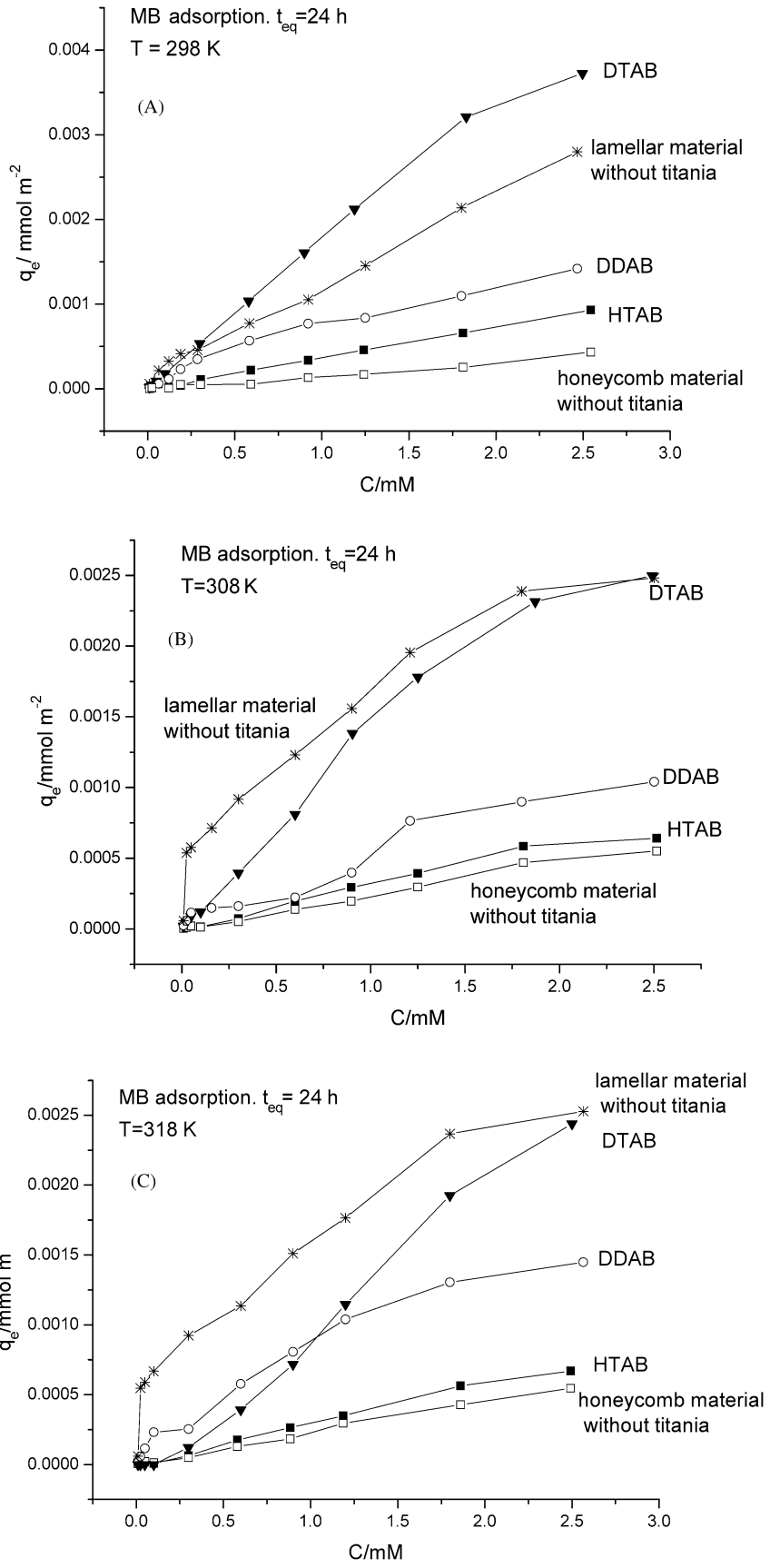

Fig. 4. Adsorption capacity variation, q_e (mmol/m^2), with initial methylene blue (MB) concentration at (A) 25, (B) 35, and (C) 45 °C. Adsorbent materials templated with (▼) DTAB, (■) HTAB, and (○) DDAB, (∗) mesoporous DDAB-templated lamellar silica material without titania, (□) mesoporous silica honeycomb material synthesized with HTAB without titania.

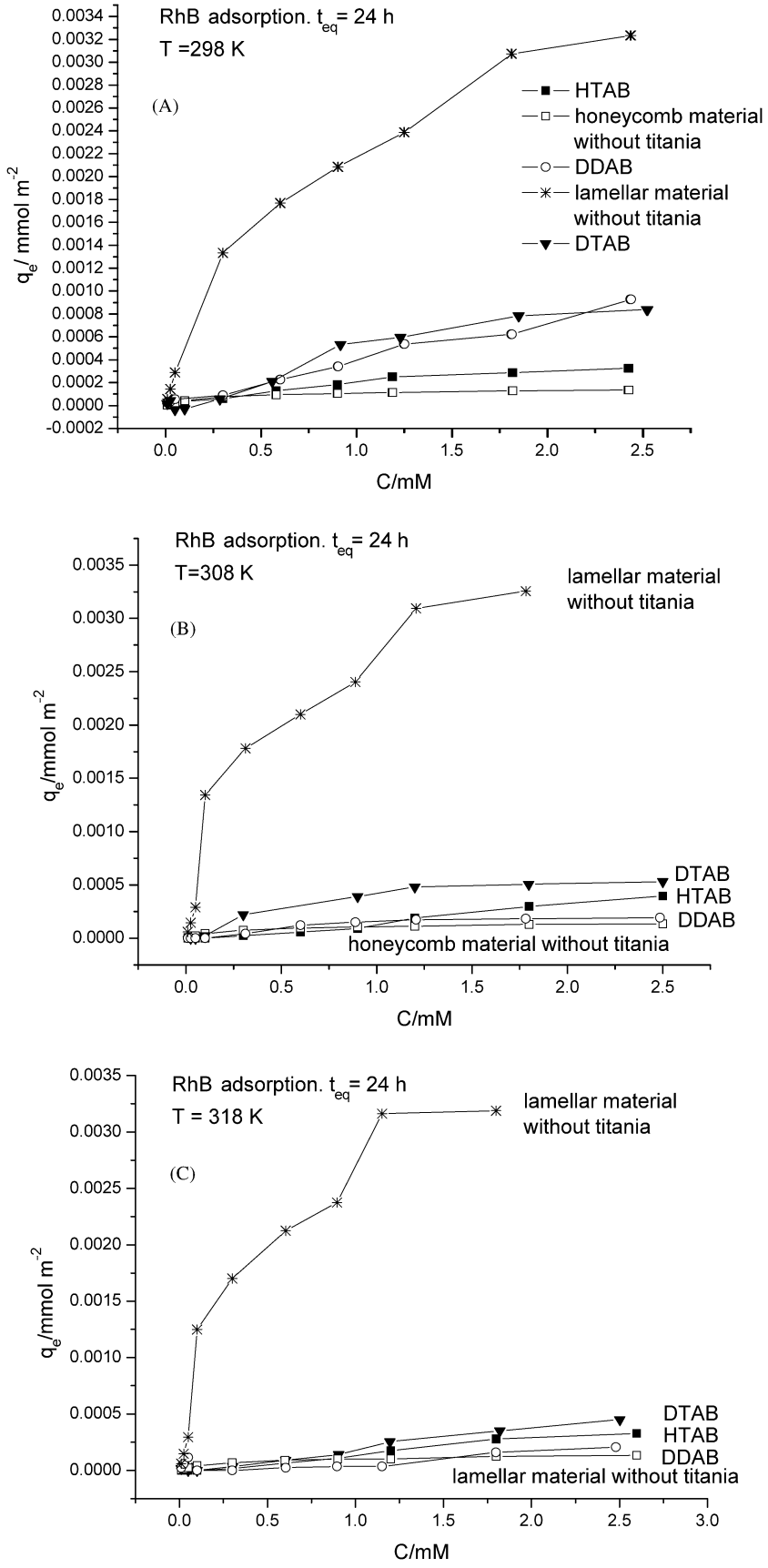

Fig. 5. Adsorption capacity variation, q_e (mmol/m^2), with initial rhodamine B (RhB) concentration at (A) 25, (B) 35, and (C) 45 °C. Adsorbent materials templated with (▼) DTAB, (■) HTAB, and (○) DDAB, (∗) mesoporous DDAB-templated lamellar silica material without titania, (□) mesoporous silica honeycomb material synthesized with HTAB without titania.

Table 2
Parameters of the Langmuir isotherm applied to the experimental data for the adsorption of MB and RhB on mesoporous adsorbents, templated with HTAB, DTAB, and DDAB, with and without titania at different temperatures

Adsorbate	Adsorbent system	q_{mon} (mmol/g)	K_L (l/mmol)	R^2
		25 °C		
MB	HTAB + TiO_2	4.79 ± 0.07	0.021 ± 0.002	1
	DTAB + TiO_2	6.27 ± 0.10	0.032 ± 0.001	1
	DDAB + TiO_2	0.07 ± 0.01	1.39 ± 0.02	0.999
	HTAB	0.07 ± 0.03	1.44 ± 0.02	0.998
	DDAB	0.19 ± 0.07	0.53 ± 0.02	0.992
	HTAB + TiO_2	0.11 ± 0.02	0.94 ± 0.02	0.945
RhB	DTAB + TiO_2	0.025 ± 0.001	4.13 ± 0.02	0.996
	DDAB + TiO_2	0.009 ± 0.007	11.21 ± 0.03	0.985
	HTAB	0.046 ± 0.008	2.24 ± 0.02	0.999
	DDAB	0.079 ± 0.012	1.29 ± 0.02	0.999
		35 °C		
MB	HTAB + TiO_2	0.06 ± 0.01	1.84 ± 0.02	0.991
	DTAB + TiO_2	0.11 ± 0.06	0.91 ± 0.01	0.998
	DDAB + TiO_2	0.019 ± 0.002	5.36 ± 0.06	0.992
	HTAB	0.08 ± 0.04	1.27 ± 0.02	0.993
	DDAB	0.042 ± 0.005	2.37 ± 0.03	0.997
	HTAB +TiO_2			
RhB	DTAB + TiO_2	0.038 ± 0.003	1.58 ± 0.07	0.997
	DDAB + TiO_2	0.045 ± 0.005	0.16 ± 0.01	0.963
	HTAB	0.05 ± 0.01	2.23 ± 0.02	0.999
	DDAB	0.12 ± 0.04	0.81 ± 0.01	0.999
		45 °C		
MB	HTAB + TiO_2	0.02 ± 0.02	5.15 ± 0.02	0.992
	DTAB + TiO_2			
	DDAB + TiO_2	0.056 ± 0.001	1.84 ± 0.02	0.998
	HTAB	0.07 ± 0.03	1.44 ± 0.02	0.998
	DDAB	0.033 ± 0.005	4.80 ± 0.82	0.993
	HTAB + TiO_2			
RhB	DTAB + TiO_2	0.035 ± 0.003	2.91 ± 0.02	0.999
	DDAB +TiO_2	0.024 ± 0.004	4.45 ± 0.02	0.998
	HTAB	0.042 ± 0.007	2.46 ± 0.03	0.999
	DDAB	0.12 ± 0.03	0.87 ± 0.01	0.999

Note. K_L and q_{mon} correspond to Eq. (3), and R^2 is the square of the correlation coefficient.

Table 3
Parameters of the Freundlich isotherm applied to the experimental data at different temperatures

Adsorbate	Adsorbent system	K_F	n	R^2
		25 °C		
MB	HTAB + TiO_2	0.09 ± 0.08	1.02 ± 0.01	0.999
	DTAB + TiO_2	0.18 ± 0.12	1.04 ± 0.02	0.995
	DDAB + TiO_2	0.03 ± 0.01	1.50 ± 0.03	0.998
	HTAB	0.054 ± 0.002	1.08 ± 0.07	0.984
	DDAB	0.032 ± 0.001	1.45 ± 0.08	0.987
	HTAB + TiO_2	0.05 ± 0.02	1.24 ± 0.01	0.951
RhB	DTAB + TiO_2	0.04 ± 0.01	1.43 ± 0.03	0.968
	DDAB + TiO_2	0.015 ± 0.001	1.62 ± 0.06	0.980
	HTAB	0.038 ± 0.001	1.36 ± 0.07	0.993
	DDAB	0.026 ± 0.001	1.66 ± 0.08	0.997
		35 °C		
MB	HTAB + TiO_2	0.09 ± 0.01	1.02 ± 0.01	0.990
	DTAB + TiO_2	0.07 ± 0.02	1.00 ± 0.03	0.997
	DDAB + TiO_2	0.022 ± 0.001	1.44 ± 0.03	0.978
	HTAB	0.054 ± 0.001	1.17 ± 0.05	0.993
	DDAB	0.032 ± 0.002	2.07 ± 0.02	0.993
	HTAB + TiO_2	0.033 ± 0.001	0.72 ± 0.01	0.995
RhB	DTAB + TiO_2	0.019 ± 0.001	1.08 ± 0.02	0.996
	DDAB + TiO_2	0.006 ± 0.001	1.50 ± 0.05	0.958
	HTAB	0.056 ± 0.003	1.65 ± 0.03	0.969
	DDAB	0.05 ± 0.01	1.25 ± 0.06	0.988
		45 °C		
MB	HTAB + TiO_2	0.070 ± 0.005	1.01 ± 0.01	0.978
	DTAB + TiO_2	0.044 ± 0.001	0.70 ± 0.01	0.995
	DDAB + TiO_2	0.019 ± 0.002	1.38 ± 0.05	0.989
	HTAB	0.052 ± 0.003	1.17 ± 0.01	0.992
	DDAB	0.030 ± 0.005	2.89 ± 0.03	0.973
	HTAB + TiO_2	0.010 ± 0.001	0.69 ± 0.01	0.979
RhB	DTAB + TiO_2	0.010 ± 0.001	0.82 ± 0.01	0.993
	DDAB + TiO_2	0.0019 ± 0.0002	0.59 ± 0.01	0.961
	HTAB	0.024 ± 0.004	1.69 ± 0.05	0.969
	DDAB	0.048 ± 0.003	1.26 ± 0.01	0.988

Note. K_F and n correspond to Eq. (5), and R^2 is the square of the correlation coefficient.

particles, it can be seen that without increasing the pore diameter or the adsorbent surface area the presence of TiO_2 augments the adsorption capacity (q_e).

This fact is due to possible degradation of the dye molecule in contact with the TiO_2 particles in the adsorbent interior. The degradation of dyes or other pollutants on TiO_2 particles or films is well documented in the literature [23,24]. Often this process is associated with UV photoinduction [25,26]. In this work the application of light was not done; the confinement of the TiO_2 particles on the silica mesoporous structure was enough to provoke the same effect.

In general, for all systems (dye + adsorbent), there was a diminution of the adsorption capacity, q_e, with the augmentation of temperature.

From the analysis of q_e vs C plots, Figs. 2–5, it was clear that the adsorption of MB in all the studied adsorbent systems is higher than of RhB. This may be due to the different molecular sizes of the two dyes. The bigger RhB molecule offers major resistance to penetration into the adsorbent mesoporous structure.

When large molecules (which also have peripheral dipoles and polar groups) are adsorbed, the dispersion forces energy is greater than the electrostatic interaction energy. As a consequence, the adsorbed molecule presents a forced dipolar orientation, since the molecule dipole axis is oriented at a certain angle with respect to the adsorbent surface electrostatic field.

The Freundlich equation predicts that the adsorption will increase monotonically with the increase of the solution dye concentration.

The Freundlich parameters, Table 3, show that the adsorption conditions in almost all cases are favorable ($n > 1$), with a higher adsorption capacity (K_F) for the MB sorption. Temperature changes altered dye adsorption. It can be seen that the increase of temperature reduces the values of n and K_F, so both adsorption capacity and favorability diminish with the temperature increment.

The adsorbent characteristics also play an important role in the adsorption process, especially if there are significant differences in their specific surface areas and porosity. Table 3 shows that the adsorption capacities for MB at 25 °C have the following order: DTAB + TiO_2 > HTAB + TiO_2 > DDAB + TiO_2.

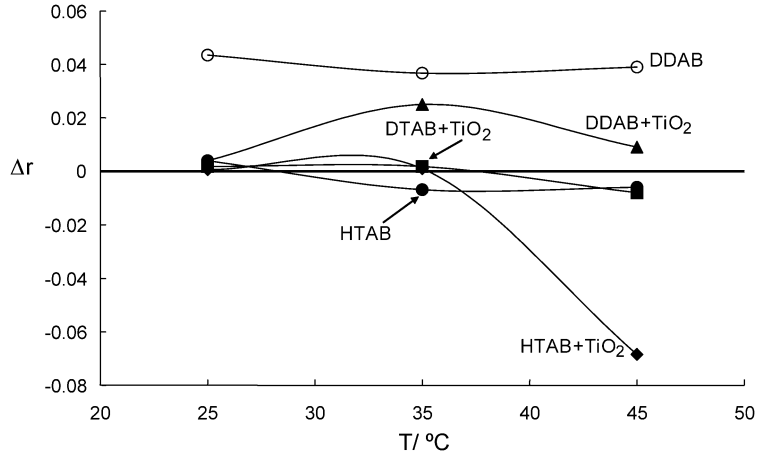

Fig. 6. Difference ($\Delta r = r_{\text{Langmuir}} - r_{\text{Freundlich}}$) between the correlation coefficient of the Langmuir and Freundlich fittings to the experimental data for MB and the different adsorbents as a function of the temperature.

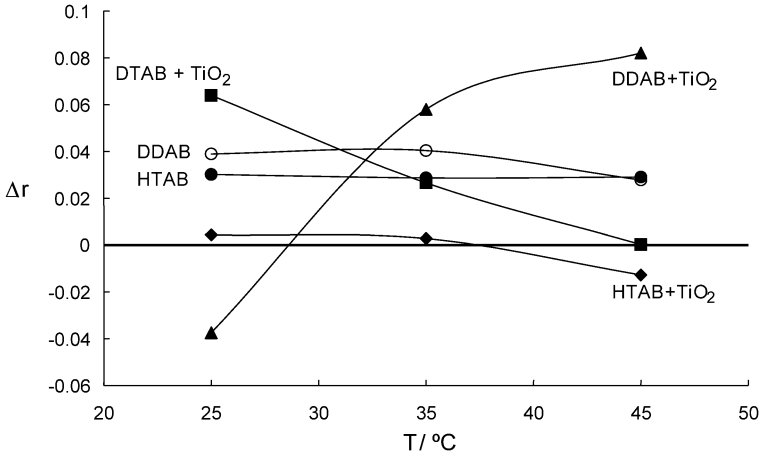

Fig. 7. Difference ($\Delta r = r_{\text{Langmuir}} - r_{\text{Freundlich}}$) between the correlation coefficients of the Langmuir and Freundlich fittings to the experimental data for RhB and the different adsorbents as a function of the temperature.

When temperature increases to 35 °C the order changes: DTAB + TiO_2 ≈ HTAB + TiO_2 > DDAB + TiO_2. At 45 °C the order is HTAB + TiO_2 > DTAB + TiO_2 > DDAB + TiO_2. With the temperature augment, the adsorption is less favored and the effect of the adsorbent specific surface becomes more evident, so the adsorbent system HTAB + TiO_2 with the greater specific surface area (272.38 m^2/g) shows the higher adsorption capacity.

For RhB adsorption the order at 25 and 35 °C, was DDAB + TiO_2 > DTAB + TiO_2 > HTAB + TiO_2, and at 45 °C it was DTAB + TiO_2 > HTAB + TiO_2 ≈ HTAB + TiO_2. In this case the effect is different. Even though the HTAB + TiO_2 adsorbent system has a greater specific surface area, its average pore diameter is smaller. Thus RhB is a reactive dye with a large molecular size, so its adsorption is favored by high-pore-diameter adsorbents, such as DTAB + TiO_2 and DDAB + TiO_2.

3.2. *Effect of temperature on the adsorption isotherm*

From the adsorption isotherm data at different temperatures, the enthalpy (ΔH^0_{ads}), entropy (ΔS^0_{ads}) and free energy of adsorption (ΔG^0_{ads}) can be calculated using the equations [27]

$$\ln K_{\text{L}} = \frac{\Delta S}{R} - \frac{\Delta H}{RT}, \tag{6}$$

$$\Delta G = \Delta H - T\Delta S, \tag{7}$$

where K_{L} is the Langmuir equilibrium constant, T is the solution temperature, and R is the gas constant. The (ΔH^0_{ads}) and (ΔS^0_{ads}) values were calculated from the slope and y-intercept of the van 't Hoff plots of $\ln K$ vs $1/T$.

The results are presented in Table 4. As seen from this table, the enthalpy of adsorption is relatively high, indicating that interaction between sorbent and adsorbate molecules is not only physical but chemical. There is a kind of chemical interaction between the adsorbent structure and dye molecules. Similar results were observed for the adsorption of MB onto anatase, which indicate a very strong interaction [28].

Such interactions depend on the type of surfaces and the compound of interests.

Dyes molecules as an organic material can adsorb via several different mechanisms because they can be either polar or nonpolar in all or part of the compound and because they may or may be not charged.

Table 4
Thermodynamic parameters of dye adsorption on the different mesoporous adsorbents

Adsorbate	Adsorbent system	(ΔH^0_{ads}) (kJ mol^{-1})	(ΔS^0_{ads}) (kJ mol^{-1})	R^2	(ΔG^0_{ads}) (kJ mol^{-1})		
					25 °C	35 °C	45 °C
MB	HTAB + TiO_2	-11.64 ± 2.04	-0.0287 ± 0.002	0.991	-3.08 ± 0.46	-2.80 ± 0.42	-2.51 ± 0.37
	DTAB + TiO_2	-56.78 ± 10.40	-0.175 ± 0.020	0.988	-4.63 ± 0.85	-2.88 ± 0.57	-1.13 ± 0.20
	DDAB + TiO_2	-21.89 ± 1.37	-0.065 ± 0.004	0.957	-2.52 ± 0.15	-1.87 ± 0.12	-1.22 ± 0.07
RhB	HTAB + TiO_2	-21.04 ± 7.17	-0.060 ± 0.014	0.948	-3.16 ± 0.79	-2.56 ± 0.64	-1.96 ± 0.49
	DTAB + TiO_2	-32.94 ± 5.14	-0.098 ± 0.013	0.956	-3.74 ± 0.56	-2.76 ± 0.41	-1.77 ± 0.26
	DDAB + TiO_2	-81.31 ± 10.75	-0.251 ± 0.030	0.998	-6.51 ± 0.86	-4.00 ± 0.60	-1.49 ± 0.22

The high adsorption enthalpy values are a result of number of chemical interactions involving electrostatic attraction, covalent bonding, nonpolar interaction, water bridging, and hydrogen-type bonding between the dye molecules and the adsorbent structure and between adsorbed dye molecules [29].

Electrostatic interaction forces between dye molecules and the adsorbent structure are clearly involved because the dyes' molecules have a positive net charge and the adsorbent SiO–TiO has a negatively charged surface (mainly due to oxygen or hydroxyls).

In addition to electrostatic interaction, there is the possibility of H-bond and water-bridge formation between the amine, carboxylate, and heterocyclic N or O groups in the adsorbate organic structure and OH group which is present at the silica–titania adsorbent surface. Hydroxyl groups are bonded to Si atoms at the Si–O–Si framework and as a consequence of the incomplete electronic Si *d* layer, the electronic density distribution in the OH groups presents a negative charge density highly displaced throughout the O atom. So a dipole is formed with the positive center located at the H atom.

Moreover, dye molecules which have highly periphery electronic displacements (peripheral dipoles, quadrupoles, and π-electronic clouds) could form H-bonds with the adsorbent surface.

The existence of H-bonds and water bridges between the adsorbent and the adsorbate augments the total interaction energy, leading to a high enthalpy of adsorption.

Furthermore, the presence of the TiO_2 semiconducting particles in the silica adsorbent structure produced a manifestation of specific electron donation interactions between the dye molecules and the mesoporous material. These interactions often give rise to other more specific and stronger ones with the possible formation of superficial chemically adsorbed complexes.

The formation of bonds between the metal atoms of the adsorbent and the adsorbed molecules produces heat, providing energy to loosen the bonds between the metal atom and its neighbors. This allows it to move from its original position and thus strengthens the chemical bond between the adsorbed molecule and the metal [30].

Figs. 8 and 9 show a schematic representation of the possible interaction between the two dye molecules and the adsorbent structure.

A last contribution to the adsorption enthalpy would be due to the adsorbate–adsorbate molecular attraction. The dipoles and quadrupoles in dye structures can orientate and favored interaction between the adsorbed molecules.

In general, for both dye molecules, the ΔH^0_{ads} values (Table 4) are higher for the lamellar adsorbents. Due to the planar structure of the dye molecules, they could intercalate between the lamellar arrangements of the adsorbent material templated with DTAB and DDAB. This fact leads to a best interaction between the adsorbent and the adsorbate, which is not possible during the adsorption on the honeycomb-structured material.

The values of ΔH^0_{ads} are more negative for RhB than for MB adsorption, probably due to the possibility of RhB forming H-bonds with the adsorbent structure and with other adsorbed molecules.

The adsorption process is exothermic and this fact explains the diminution of adsorption capacity with the augment of T.

The positive adsorption entropy indicates a decrease of disorder. This fact may be related to the extent of hydration of cationic dye molecules. The reorientation or restructuring of water around dyes is very unfavorable in terms of entropy, because it disturbs the existing water structure and imposes a new and more ordered structure at the solid–solution interface during the dye adsorption [31].

Negative values of ΔS^0_{ads} suggests that enthalpy is responsible for making the ΔG^0_{ads} negative, so that the adsorption process is spontaneous though the enthalpy contribution is much larger than that of the entropy.

To analyze the entropy values, a rough computation of the entropy involved in the adsorption was made. The adsorption was assumed as change transference of q_e moles of the adsorbate from the initial solution having a concentration C_0 to a concentrated solution having q_e moles of the adsorbate in a volume equal to the surface of the adsorbent multiplied by the height H or the adsorbate molecule. With a model of the MB molecule, and supposing that the plane of the molecule is perpendicular to the adsorbent surface and its longest axis parallel to the same surface, $H = 7.04$ Å. We made the computations for the HTAB + TiO_2 system with an intermediate concentration $C_0 = 0.006$ mol dm^{-3}, with $q_e = 0.03481$ mmol g^{-1}. Computations gave the concentration at the adsorbed monolayer $C_{ads} = 0.182$ mol dm^{-3}. Thus the change in entropy because of the change of concentration was $\Delta S_{ads} = -R \ln C_{ads}/C_0 = -28.6$ J/(K mol). Some computations with other experimental data gave similar results. Note that this is the more conservative supposition, because if the MB molecule is assumed to have its plane parallel to the adsorbent surface, then the width of the monolayer is about 2.9 Å and $\Delta S_{ads} = -35.7$ J/(K mol). This means that the very small experimen-

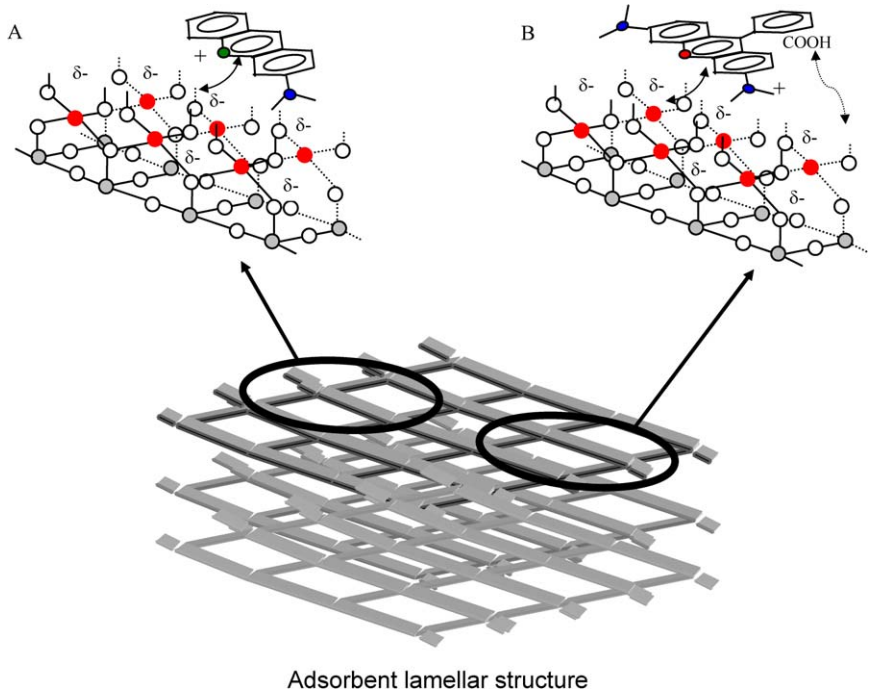

Fig. 8. Schematic representation of (A) MB and (B) RhB interaction with the surface of a lamellar adsorbent. Gray circles correspond to Si, white circles to O, and black circles to Ti. The black continuous arrow symbolizes electrostatic interaction and the noncontinuous arrow indicates H-bond.

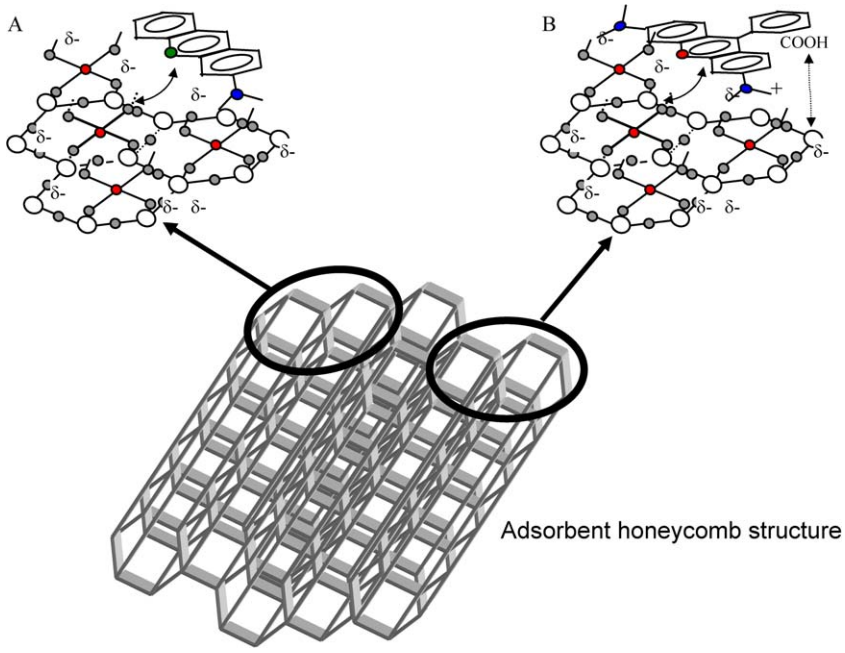

Fig. 9. Schematic representation of (A) MB and (B) RhB interaction with the surface of a honeycomb adsorbent. Symbols are the same as in Fig. 8.

tal entropies of adsorption indicate that the dye adsorption is probably accompanied by a dehydration that liberates water molecules, thus increasing the overall entropy change and compensating for the loss of freedom caused by the dye adsorption.

To compute the area occupied by a dye molecule (a_{molec}) with its plane parallel to the adsorbent surface, a scale model of each dye molecule was made. The area occupied by a MB molecule was calculated to be about 61.5 Å^2 and that of a RhB molecule to be about 144.3 Å^2. The effective area per molecule for each dye/adsorbent combination and at the three temperatures employed was computed at the maximum coverage of adsorbent

$$a_{\text{molec}} = m_{\text{adsorbent}} A_{\text{BET}} / q_{\text{mon}} N_{\text{A}}, \tag{8}$$

where N_A is the Avogadro constant. Results for MB are plotted for each adsorbent as a function of temperature in Figs. 10 and 11 for RhB. For comparison, the area per molecule estimated from the dyes structure is also represented in the figures.

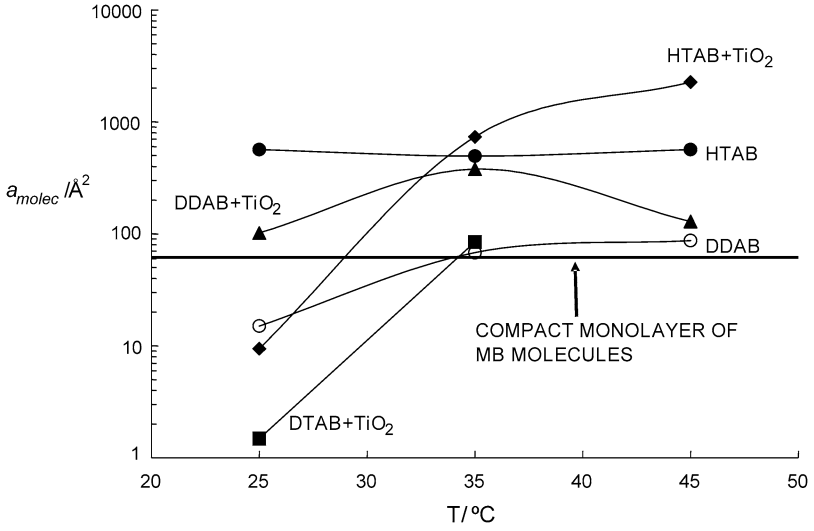

Fig. 10. Area per adsorbed MB molecule on the different adsorbents as a function of temperature.

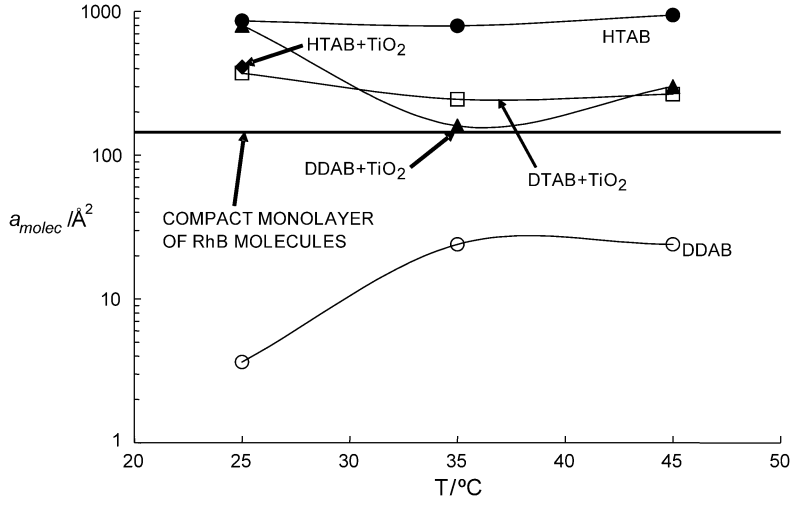

Fig. 11. Area per adsorbed RhB molecule on the different adsorbents as a function of temperature.

Fig. 10 shows the diverse behavior of MB in the different adsorbents. HTAB-templated adsorbent seems not to modify the adsorption with temperature. The monolayer is not compact. This may be caused by the heterogeneity of the surface, formed by negatively charged and uncharged groups. Another explanation may rely on the small size of some pores. From Table 1, the average pore diameter of the HTAB-templated mesoporous material is 4.55 Å, whereas the smaller dimension of the MB molecule is $H = 7.04$ Å. So a large proportion of the BET surface area may be unattainable for the MB molecules and the situation may be that the external surface is completely covered by dye molecules while the cylindrical pores remain free of MB molecules. The experimental a_{molec} values are compatible with MB molecules being situated with their planes parallel to the adsorbent surface. The same situation is compatible with the a_{molec} values for the system DDAB + TiO_2 at all temperatures, and the other systems at 35 and 45 °C. However, at 25 °C some systems show a_{molec} values that are incompatible with the MB molecules packing image at the monolayer. These systems have larger pores than the HTAB-templated ones. Moreover, in the DDAB, DDAB + TiO_2, and DTAB + TiO_2 systems, the pores are slit-shaped. In these systems, the MB molecules may be situated with their planes perpendicular to the adsorbent surface. This situation may not be more energetically convenient and the increase of temperature may cause a partial desorption resting at the interface with only the most energetically anchored molecules.

Fig. 11 shows the a_{molec} results for RhB. Except for the DDAB-templated system, all the adsorbents show a noncompact monolayer compatible with the molecule resting with its plane parallel to the adsorbent surface. The DDAB system is lamellar and the RhB molecules may be situated sandwiched between the silica lamellae with their plane perpendicular to the adsorbent surface. It also must be remembered that the RhB molecules are bigger than MB ones. The smallest axis of the molecule in the plane is $H = 15.3$ Å, which is larger than all the measured pore diameters. So these systems may have the external surface completely covered by dye molecules while their pores remain free of dye molecules.

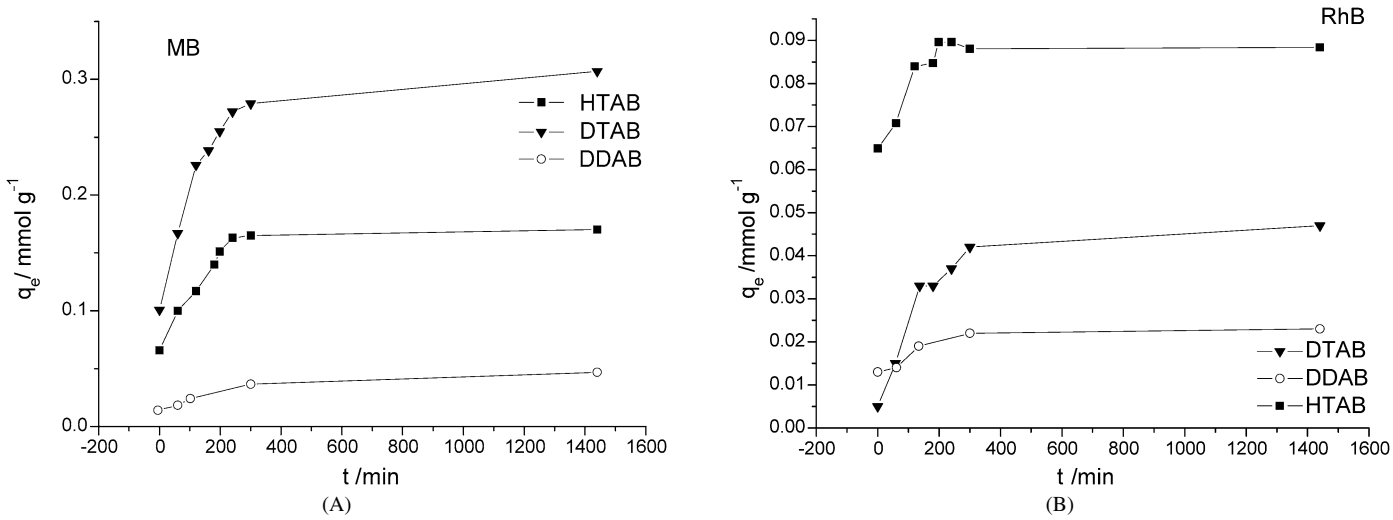

Fig. 12. Variation of q_e vs time for (A) MB and (B) RhB adsorption at 25 °C. Silica–titania composed adsorbent materials templated with (▼) DTAB, (■) HTAB, and (○) DDAB.

3.3. Adsorption kinetic

Fig. 12 shows the influence of contact time on dye removal by the three adsorbent systems at 25 °C; similar plots were obtained for 35 and 45 °C. Three consecutive mass transport steps are associated with the adsorption of solute from solution by porous adsorbent [32]. First, the adsorbate migrated thought the solution to the external surface of the adsorbent particles by molecular diffusion, i.e., film diffusion, followed by solute movement from the particles surface into internal sites by pore diffusion and finally the adsorbate is adsorbed onto active sites at the interior of the adsorbent particles. This phenomenon takes relatively long contact time.

The kinetic adsorption data were processed to understand the dynamics of the adsorption process in terms of the order, n, and of the rate constant, k, according to the equation

$$v = \frac{dq_e}{dt} = -kq_e^n, \tag{9}$$

$$\log v = \log k - n \log q, \tag{10}$$

where v is the rate of adsorption and q_e the adsorption capacity.

The logarithmic variation of v vs $\log q_e$ was shown for the MB adsorption in Fig. 13, n and k were calculated from the slope and y-intercept of the graph. Similar results were obtained for RhB adsorption.

According to the obtained values of n, Table 5, kinetic data were treated with the pseudo-first-order kinetic model [33]

$$\frac{dq_t}{dt} = k_1(q_e - q_t), \tag{11}$$

where q_e and q_t refer to the amount of dye adsorbed (mmol/g) at equilibrium and at any time t (min), respectively, and k_1 is the equilibrium rate constant of pseudo-first-order sorption (min^{-1}). Integrating Eq. (11) for the boundary conditions $t = 0$ to t and $q_t = 0$ to q_t gives

$$\log \frac{q_w}{q_e - q_t} = \frac{k_1}{2.303}t, \tag{12}$$

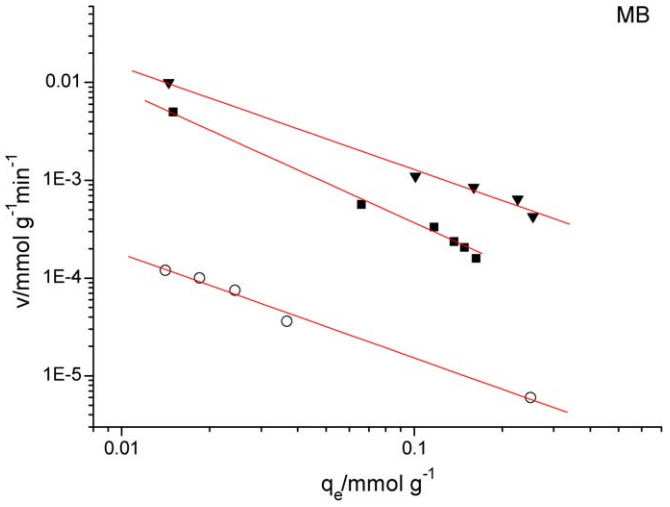

Fig. 13. Variation of the MB adsorption rate at 25 °C. Silica–titania adsorbent materials templated with (▼) DTAB, (■) HTAB, and (○) DDAB. Similar results were obtained for the RhB adsorption.

which is the integrated law for a pseudo-first-order reaction. Equation (12) can be rearranged to obtain a linear form:

$$\log(q_e - q_t) = \log q_e - \frac{k_1}{2.303}t, \tag{13}$$

Values of the rate constant, k_1, equilibrium adsorption capacity, q_e, and correlation coefficient, r_1^2, were calculated from the plots of $\log(q_e - q_t)$ vs t, Fig. 14, for both dye solution samples and summarized in Table 6. The adsorption kinetic is not significantly affected by the variation of T.

The correlation coefficients for MB and RhB adsorption on the three adsorbent systems are found to be higher than 0.98 and the calculated equilibrium adsorption capacities are agreed with experimental values.

The obtained k_1 values for MB adsorption indicates that the adsorption rate increases as the adsorbent surface area augments (HTAB > DTAB > DDAB templated materials).

Table 5
Kinetic adsorption parameters obtained using Eq. (11)

Adsorbate	Adsorbent system	n	k_1 (min^{-1})	R^2
		$T = 25\,°C$		
MB	HTAB + TiO_2	1.33 ± 0.18	0.016 ± 0.001	0.984
	DTAB + TiO_2	0.91 ± 0.24	0.0072 ± 0.0010	0.996
	DDAB + TiO_2	1.26 ± 0.19	0.006 ± 0.002	0.986
		$T = 35\,°C$		
	HTAB + TiO_2	1.23 ± 0.16	0.012 ± 0.001	0.994
	DTAB + TiO_2	1.11 ± 0.22	0.0070 ± 0.0010	0.986
	DDAB + TiO_2	1.16 ± 0.10	0.0051 ± 0.0021	0.989
		$T = 45\,°C$		
	HTAB + TiO_2	1.32 ± 0.15	0.010 ± 0.001	0.994
	DTAB + TiO_2	0.97 ± 0.21	0.0068 ± 0.0010	0.996
	DDAB + TiO_2	0.96 ± 0.16	0.0062 ± 0.0012	0.996
		$T = 25\,°C$		
RhB	HTAB + TiO_2	0.64 ± 0.02	0.0288 ± 0.003	0.998
	DTAB + TiO_2	1.32 ± 0.24	0.0127 ± 0.002	0.969
	DDAB + TiO_2	0.95 ± 0.15	0.0095 ± 0.0010	0.982
			$T = 35\,°C$	
	HTAB + TiO_2	0.74 ± 0.01	0.020 ± 0.002	0.981
	DTAB + TiO_2	1.12 ± 0.24	0.016 ± 0.001	0.986
	DDAB + TiO_2	0.90 ± 0.11	0.010 ± 0.001	0.983
		$T = 45\,°C$		
	HTAB + TiO_2	0.94 ± 0.02	0.0235 ± 0.003	0.981
	DTAB + TiO_2	1.02 ± 0.24	0.0157 ± 0.0001	0.988
	DDAB + TiO_2	0.95 ± 0.25	0.0095 ± 0.0004	0.987

For RhB adsorption process, the k_1 values are bigger than the obtained for MB. This fact is probably due to the possibility of H-bond formation between RhB molecules and the adsorbent surface. Furthermore, being RhB a big molecule its adsorption is limited by it size, so the effect of the adsorbent surface area is in this case not very evident.

Kinetic data were further treated with a pseudo-second-order kinetic model [33,34]. The obtained results, not shown, indicated that this model does not agree with experimental values.

4. Summary

The sorption of two basic reactive dyes, methylene blue (MB) and rhodamine B (RhB), from aqueous solution onto three different mesoporous adsorbent systems containing TiO_2 particles was studied in this work.

The variation of adsorption capacity (q_e), Eq. (2), indicated a great dependence of the adsorption mechanisms on the adsorbent structure, the dyes' molecular configuration, and the temperature conditions.

In general, for all systems (dye + adsorbent), there was a diminution of the adsorption capacity, q_e, with the augment of temperature. The effect was higher for the adsorption on the DTAB templated material.

It was clear that the adsorption of MB in all the proved adsorbent systems was higher than that of RhB. The effect may be due to the larger molecular size of RhB than MB, which may render unattainable the pore interior of adsorbents for the dye molecules. So, in many cases, the external surface may be covered with dye molecules, whereas the pores may remain free of adsorbate.

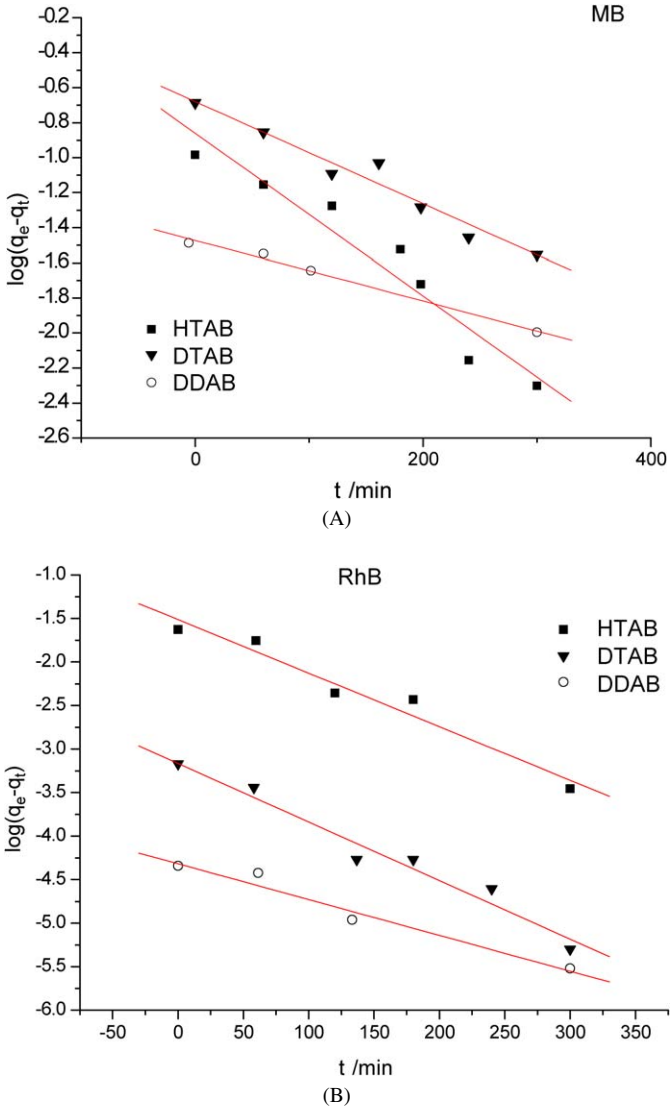

Fig. 14. Kinetic first-order model representation of (A) MB and (B) RhB adsorption at 25 °C. Silica–titania adsorbent materials templated with (▼) DTAB, (■) HTAB, and (○) DDAB.

To determine the mechanism of dye adsorption and evaluate the effect of temperature on adsorption capacity, the experimental data were treated with the Langmuir and Freundlich isotherm equations. The analysis of the obtained parameters and correlation coefficients for both models showed that the adsorption of the two reactive dyes (MB and RhB) on the three proved silica–titania adsorbent systems at the three work temperatures was best fitted by the employment of the Langmuir model. The Freundlich parameters showed that in general the adsorption conditions were favorable ($n > 1$), with a higher adsorption capacity (K_F) for the MB sorption.

The change of temperature affected dye adsorption. The increase of temperature reduced the values the n and K_F, so adsorption capacity and favorability diminished. In the particular case of RhB adsorption, the augmentation of T leads to unfavorable adsorption with $n < 1$, Table 3.

The temperature effect was also used to calculate the enthalpy, entropy, and free energy of adsorption. The analysis of

Table 6
Kinetic adsorption parameters obtained using Eq. (10)

Adsorbate	Adsorbent system	Order	q_e (mmol/g)	q_e* (mmol/g)	k_1 (min^{-1})	R^2
			$T = 25\,°C$			
MB	HTAB + TiO_2	1	0.17	0.140 ± 0.002	0.011 ± 0.001	0.986
	DTAB + TiO_2	1	0.30	0.210 ± 0.010	0.0068 ± 0.0030	0.985
	DDAB + TiO_2	1	0.041	0.046 ± 0.001	0.0039 ± 0.0010	0.997
			$T = 35\,°C$			
	HTAB + TiO_2	1	0.174	0.151 ± 0.004	0.0108 ± 0.002	0.982
	DTAB + TiO_2	1	0.14	0.200 ± 0.009	0.007 ± 0.001	0.985
	DDAB + TiO_2	1	0.045	0.045 ± 0.001	0.0041 ± 0.0001	0.991
			$T = 45\,°C$			
	HTAB + TiO_2	1	0.18	0.17 ± 0.04	0.0105 ± 0.001	0.981
	DTAB + TiO_2	1	0.136	0.16 ± 0.01	0.0066 ± 0.001	0.992
	DDAB + TiO_2	1	0.054	0.047 ± 0.003	0.0039 ± 0.0004	0.985
			$T = 25\,°C$			
RhB	HTAB + TiO_2	1	0.088	0.030 ± 0.002	0.014 ± 0.001	0.989
	DTAB + TiO_2	1	0.047	0.041 ± 0.001	0.0157 ± 0.002	0.983
	DDAB + TiO_2	1	0.024	0.014 ± 0.002	0.0095 ± 0.0010	0.982
			$T = 35\,°C$			
	HTAB + TiO_2	1	0.13	0.14 ± 0.005	0.012 ± 0.002	0.981
	DTAB + TiO_2	1	0.035	0.040 ± 0.001	0.016 ± 0.001	0.986
	DDAB + TiO_2	1	0.029	0.016 ± 0.003	0.010 ± 0.001	0.983
			$T = 45\,°C$			
	HTAB + TiO_2	1	0.089	0.029 ± 0.004	0.0135 ± 0.003	0.981
	DTAB + TiO_2	1	0.034	0.038 ± 0.001	0.0157 ± 0.0001	0.988
	DDAB + TiO_2	1	0.026	0.014 ± 0.004	0.0095 ± 0.0004	0.987

* Calculated from kinetic data.

these thermodynamic parameters suggested that the adsorption is mainly chemical because of the high adsorption enthalpy, and that it is accompanied by strong dehydration of the adsorbate because of the low negative value of the adsorption entropy.

The kinetics of adsorption was also studied and the results followed a first-order model. The obtained k_1 values for MB adsorption indicated that the adsorption rate increased as the adsorbent surface area augmented (HTAB > DTAB > DDAB-templated materials).

For RhB adsorption process, the k_1 values were higher than those obtained for MB. This fact was probably due to the possibility of H-bond formation. Furthermore, RhB being a big molecule, its adsorption was limited by its size to the external surfaces of the adsorbent, so the effect of the adsorbent surface area was in this case not very evident.

The adsorption kinetic was not significantly affected by the variation of T.

Acknowledgments

This work was financed by Banco Río and PIP No. 2739 of CONICET. P.M. is an assistant researcher of the Consejo Nacional de Investigaciones Científicas y Técnicas de la República Argentina (CONICET).

References

[1] K.R. Ramakrishna, T. Viraraghavan, Water Sci. Technol. 36 (1997) 189.
[2] S. Netpradit, P. Thiravetyan, S. Towprayoon, Water Res. 38 (2004) 71.
[3] C. Moran, M.E.
[4] M.F. Boeniger, Carcinogenicity of Azo Dyes Derived From Benzidine, Department of Health and Human Services (NIOSH), Cincinnati, 1980, Pub. No. 8-119.
[5] Kirk-Othomer, Encyclopedia of Chemical Technology, eighth ed., 1994, pp. 547–672.
[6] Z.Y. Xu, Q.X. Zhang, H.H.P. Fang, Crit. Rev. Environ. Sci. Technol. 33 (2003) 1.
[7] M.M. Nassar, in: Proceedings of the International Meetings on Chemical Engineering and Biotechnology, ACHEMA-94, Frankfurt, 1994, pp. 5–11.
[8] M.M. Nassar, M.S. El-Geundi, J. Chem. Technol. Biotechnol. 50 (1991) 257.
[9] H.M. Asfour, O.A. Fadali, M.M. Nassar, M.S. El-Geundi, J. Chem. Technol. Biotechnol. 35 (1985) 28.
[10] M.S. El-Geundi, Water Res. 25 (3) (1991) 271.
[11] G. McKay, S.J. Allen, J. Sep. Process Technol. 4 (3) (1983) 1.
[12] (a) D.Y. Zhao, P.D. Yang, N. Melosh, J. Feng, B.F. Chmelka, G.D. Stucky, Adv. Mater. 10 (1998) 1380;
(b) D.Y. Zhao, P.D. Yang, D.I. Margolese, B.F. Chmelka, G.D. Stucky, Chem. Commun. (1998) 2499.
[13] Y. Lu, B. Ganguli, C.A. Drewien, M.T. Anderson, C.J. Brinker, W. Gong, Y. Guo, H. Soyez, B. Dunn, M.H. Huang, J.I. Zink, Nature 389 (1997) 364.
[14] D. Grosso, A.R. Balkenende, P.A. Albouy, M. Lavergne, L. Mazerolles, F. Babonneau, J. Mater. Chem. 10 (2000) 2085.
[15] S.D. Mo, W.Y. Ching, Phys. Rev. B 51 (1995) 13023.
[16] D.W. Kim, N. Enomoto, Z. Nakagawa, J. Am. Ceram. Soc. 79 (1996) 1095.
[17] T. Watanabe, A. Nakajima, R. Wang, M. Minabe, S. Koizumi, A. Fujishima, K. Hashimoto, Thin Solid Films 351 (1999) 260.
[18] P. Messina, M.A. Morini, M.B. Sierra, P.C. Schulz, J. Colloid Interface Sci. (2005), in press.
[19] Q.S. Huo, D.I. Margolese, V. Ciesta, P.Y. Feng, T.E. Gier, P. Sieger, R. Leon, P.M. Petroff, F. Schuth, G.D. Stucky, Nature 36 (1994) 317.
[20] I. Langmuir, J. Am. Chem. Soc. 38 (11) (1916) 2221.
[21] H. Freundlich, Z. Phys. Chem. A 57 (1906) 228.
[22] A.W. Adamson, A.P. Gast, Physical Chemistry of Surfaces, sixth ed., Wiley, New York, 1998, pp. 393–394.

[23] D. Chatterjee, A. Mahata, J. Photochem. Photobiol. A Chem. 153 (2002) 199.
[24] T. Sumita, T. Yamaki, S. Yamamoto, A. Miyashita, Appl. Surf. Sci. 200 (2002) 21.
[25] T. Tsumura, N. Kojitani, H. Umemura, M. Toyoda, M. Inagaki, Appl. Surf. Sci. 196 (2002) 429.
[26] O. Horváth, E. Bodnár, J. Hegyi, Colloids Surf. A Physicochem. Eng. Aspects 265 (2005) 135.
[27] M.S. Chiou, H.Y. Li, Chemosphere 50 (2003) 1095.
[28] M.E. Zawadski, A.W. Adamson, Foundations on Adsorption: Engineering Foundation, New York, 1987, p. 619.
[29] P. Somasundaran, S. Shrotri, L. Huang, Pure Appl. Chem. 70 (3) (1998) 621.
[30] G.A. Somorjai, W.J. Thomas, Principles and Practice of Heterogeneous Catalysis, Wiley–VCH, Berlin, 1997.
[31] A. Gürses, S. Karaca, Ç. Doğar, R. Bayrak, M. Açikyildiz, M. Yalçin, J. Colloid Interface Sci. 269 (2004) 310.
[32] S. Lagergren, K. Sven, Vetensk. Handl. 24 (4) (1898) 1.
[33] Y.S. Ho, G. McKay, Water Res. 34 (3) (2000) 735.
[34] Y.S. Ho, G. McKay, Process Biochem. 34 (5) (1999) 451.